Time Stretching of 102-GHz Millimeter Waves Using Novel 1.55-μm Polymer Electrooptic Modulator

D. H. Chang, H. Erlig, M. C. Oh, C. Zhang, W. H. Steier, L. R. Dalton, and H. R. Fetterman

***Abstract*—Millimeter (MM)-wave signals at frequencies up to 102 GHz have been time stretched down to 11 GHz using a new wide-band traveling-wave polymer modulator. This is the first application of electrooptic modulators fabricated using the new polymer material PC-CLD, which has demonstrated good optical insertion loss and high nonlinearity at 1.55 μm.**

***Index Terms*—A/D conversion, electrooptic modulators, PC-CLD, photonic time stretch, polymer modulators.**

I. Introduction

THE ELECTROOPTIC modulator is an enabling component in many photonic and optical/millimeter (MM)-wave systems. As such, its bandwidth often dictates the range of applications which are feasible. Conventional $LiNbO_3$ modulators suffer from a large microwave to optical refractive index mismatch which limits their bandwidth. Polymer modulators have demonstrated promising high-frequency performance, with modulation response from dc out to 110 GHz [1]. Recently, modulators fabricated using the new polymer material PC-CLD have shown significantly reduced optical loss and high nonlinearity at 1.55 μm [2]. As an initial demonstration of its high-frequency capabilities, we have employed time stretch to detect modulation at frequencies up to 102 GHz. Time stretch utilizes linear group velocity dispersion in optic fibers to frequency downshift microwave signals modulated onto optical pulses. The technique has been proposed as a signal preprocessor to extend the upper frequency range of electronic analog/digital (A/D) converters, and has been demonstrated in [3].

Time stretch is related to frequency shifting of modulated optical pulses using time lenses [4], [5]. Time-lens action on electrical signals was also demonstrated earlier in [6]. Unfortunately, the authors of both [3] and [6] use the name "stretch," which can be a source of confusion. The fundamental difference between the two techniques is whether the temporal analog of the imaging condition is obeyed [7]. In [4]–[6], the imaging condition is fulfilled by the use of a quadratic phase (linear frequency) modulation element, which is the analog of a spatial thin lens. In the technique used in [3] and here, temporal magnification relies on dispersion alone. The spatial analog is simply a transparency held before a narrow beam, with the dispersive elements being the space between the beam source, the transparency, and the screen. This greatly simplifies implementation, but incurs a penalty which is analogous to that of an unfocused spatial imaging system. High frequencies are attenuated, imposing a bandwidth limitation which increases in severity with increasing magnification [3].

Manuscript received November 29, 1999; revised February 9, 2000. This work was supported under grants from the AFOSR and DARPA.

D. H. Chang and H. R. Fetterman are with the Department of Electrical Engineering, University of California at Los Angeles, Los Angeles, CA 90095 USA (e-mail: dhchang89@alum.mit.edu).

H. Erlig is with Pacific Wave Industries, Los Angeles, CA 90024 USA.

M. C. Oh, C. Zhang, W. H. Steier, and L. R. Dalton are with the Department of Electrical Engineering and Chemistry, University of Southern California, Los Angeles, CA 90098 USA.

Publisher Item Identifier S 1041-1135(00)03685-2.

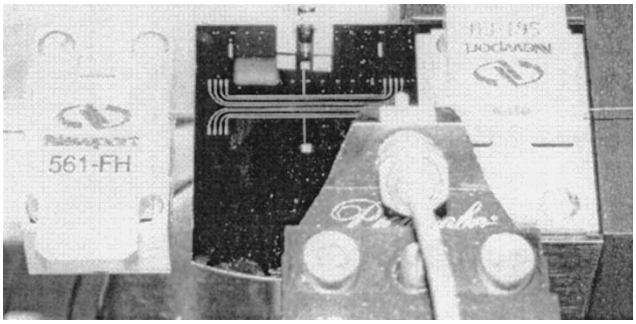

Fig. 1. PC-CLD polymer modulator in experimental setup with fiber coupling and V-band microwave probe. Light is coupled into and out of the modulator using fibers tipped with cylindrical lenses, which minimizes the coupling loss to about 1.5 dB/facet.

II. The PC-CLD Modulator

Fig. 1 shows the experimental unpackaged PC-CLD modulator used here. The substrate is gold-plated silicon, onto which the active material is spun and corona poled. Ridge optical waveguides are fabricated into the active material to form Mach–Zehnder interferometers (MZI's). The substrate serves as the ground plane for the microstrip lines patterned above the optical waveguides. Details on the fabrication and characterization of the device are discussed in [2]. The modulating electrical signal is injected from a coplanar probe near the input fiber. The probe shown is rated to 67 GHz; for modulation at 102 GHz, one with a W-waveguide input is substituted.

Figures of merit for the PC-CLD modulator are preliminary, as key elements such as interaction length and microstrip design are being optimized. Measurements conducted on this particular sample shows $V_\pi \approx 5$ V and total insertion loss of 12 dB. The device shows a flat frequency response to 40 GHz. Although operation well above 40 GHz has been demonstrated (for example in this experiment), a detailed frequency response measurement remains to be performed. While the device has survived repeated operation at 5–10 mW of optical power, long-term power limitations will be established once packaged units with fiber-pigtails are fabricated.

III. Time-Stretch Theory

Time stretch exploits group velocity dispersion (GVD) to temporally expand a pulse while preserving its envelope shape. Details of the theory are in [3]. Two long fiber spools of length L_1 and L_2 are used, with the modulator in between. The relevant stretch factor M is the width of the pulse exiting L_2 compared to that exiting L_1. If we denote by τ_0 the pulse width exiting the laser and $\delta\tau_1$, $\delta\tau_2$ the additional broadening from L_1, L_2, respectively, then

$$M = \frac{\tau_0 + \delta\tau_1 + \delta\tau_2}{\tau_0 + \delta\tau_1} = 1 + \frac{\delta\tau_2}{\tau_0 + \delta\tau_1} \approx 1 + \frac{L_2}{L_1} \qquad (1)$$

if $\tau_0 \ll \delta\tau_1$. This is certainly true in our system, where τ_0 (autocorrelation) ≈ 150 fs, while $\tau_0 + \delta\tau_1 > 1$ ns.

IV. Experimental Results

The optical source is a passively mode-locked Er^{3+}-doped fiber laser with a 50-nm pulse bandwidth at 1.55 μm and a 40-MHz repetition rate. To ensure linear propagation, the optical power is attenuated with a combination of neutral-density plates and variable attenuator. The output of the attenuator is propagated through L_1 (standard SMF) and a fiber-polarization controller before entering the modulator. The modulated output is amplified in an Er^{3+}-doped fiber amplifier before entering the L_2 spools, also SMF. The output of the L_2 spools is detected by a 45-GHz bandwidth photodiode and amplified by a 32-dB microwave amplifier. The specified passband of the amplifier is 8–12 GHz.

Four modulation sources are used: a sweep oscillator (to 40.8 GHz), a synthesizer (to 50 GHz), a GUNN oscillator (61.2 GHz), and a Klystron (102 GHz). Data are captured with both a spectrum analyzer and a sampling oscilloscope. To see the effect of time stretching directly in the time domain would require locking the laser pulse rate to the modulating source, an unavailable option for the last three sources. We instead rely on an indirect signature in the frequency domain, since the basic operation of time stretching has already been demonstrated [3]. The combined effect of modulation and subsequent time stretching is a frequency shifting of the carrier pulses' power spectral density to the stretched modulation frequency, which is observable using the spectrum analyzer.

Fig. 2 shows the unmodulated pulse after traversing the entire system, with $L_1 = 1.5$ and $L_2 = 4.5$ km. As can be seen, the pulse is much wider than its initial 150-fs width, and has acquired ripples which translate to "twin lobes" in the power spectral density. A fast Fourier transform (FFT) performed on the time-domain pulse corroborates the spectrum analyzer data. The source of the ripples has been isolated to the slight effective length mismatch between the two arms of the MZI. While such a mismatch is routinely compensated for with a bias voltage when modulating a CW beam, it produces intensity ripples in a highly chirped pulse. The ripple period is a function of the chirp parameter and the effective temporal mismatch. In addition, since waves of different polarizations in the optical waveguide suffer different mismatches, the overall output pulse shape is highly sensitive to the input polarization.

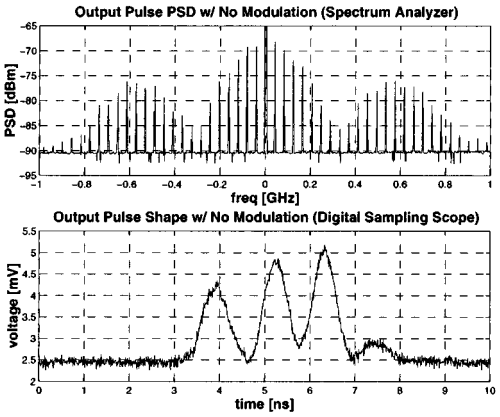

Fig. 2. Pulse power spectral density (PSD) and temporal shape with no modulation. The spike at dc is due to the noise floor.

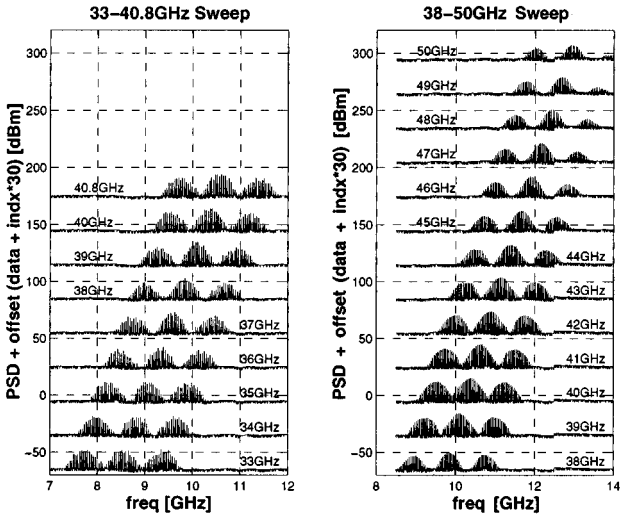

Fig. 3. Spectrum analyzer data for two modulation frequency sweeps. The spectra are replicas of that in Fig. 2 shifted to the stretched modulation frequency.

In an A/D application, the pulse ripples compete with the modulated signal and would be an undesirable feature which must be eliminated in postprocessing at the expense of conversion accuracy. For this experiment, no such compensation is required to recognize the effect of modulation, which simply frequency shifts the entire PSD waveform. The spacing between the PSD spectral lines is equal to the 40-MHz laser repetition rate, as expected.

Fig. 3 shows the shifted spectra as the modulation frequency is swept from 33 to 50 GHz, with $L_1 = 1.5$ and $L_2 = 4.5$ km. The centers of the captured spectra are extracted and plotted against the modulation frequency in Fig. 4. As expected, the relationship is linear; the fitted M is 3.86. The "upper lobes" of the spectra near 50 GHz are distorted by the bandwidth of the 8–12-GHz microwave amplifier.

In Fig. 5, a GUNN oscillator with a measured peak at 61.8 GHz is used to drive the modulator. To bring the stretched waveform back into the microwave amplifier's passband, L_2 is increased to 6.5 km, while L_1 remains at 1.5 km. In all other aspects, the system remains unchanged from the 33- to 50-GHz data set. The measured M is 5.13.

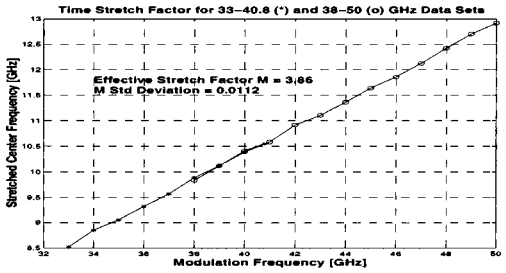

Fig. 4. Effective stretch ratio calculated for data sets seen in Fig. 3. From the data, $M_{\text{eff}} = 3.86$, with a 1σ deviation from linearity of 1.1%. The calculated value from (1) is $M = 4$.

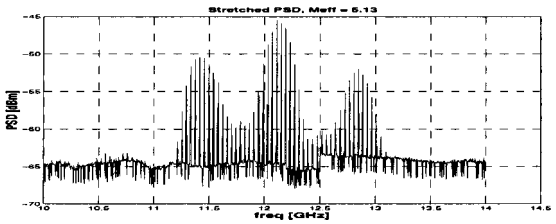

Fig. 5. GUNN-oscillator source with output measured at 61.81 GHz is time stretched to 12.05 GHz ($M = 5.13$). The pulse shape remains similar to that in Fig. 3.

Finally, time stretch using a Klystron oscillator at 101.7 GHz (as measured by a frequency counter and harmonic mixer) is shown in Fig. 6. Now $L_1 = 0.5$ and $L_2 = 5.0$ km to bring M to 11; the measured ratio is 9.8. The large change in fiber arrangement alters the pulse shape, as can be inferred by the zero-modulation PSD in Fig. 6. With the signal level available, only the top portion rises above the noise floor in the stretched data.

The discrepancies between measured and calculated stretch ratios stem from dispersion introduced ahead of the modulator by the variable attenuator and a 50-m fiber patch cord connecting the laser to the L_1 spool. The effective M from (1) is

$$M_{\text{eff}} = 1 + \frac{L_2}{L_1 + \delta}$$

where δ represents dispersion equivalent to that length of SMF. Solving for δ in the three frequency regimes using measured M_{eff}'s of 3.86, 5.13, and 9.80 gives self-consistent values of 73, 74, and 68 m, respectively.

V. Conclusion

This experiment is the first reported application of electrooptic modulators fabricated from the new polymer material PC-CLD. We have utilized time stretching to show modulation at up to 102 GHz. It extends the previously demonstrated high-frequency capabilities of polymer modulators to important 1.55-μm applications.

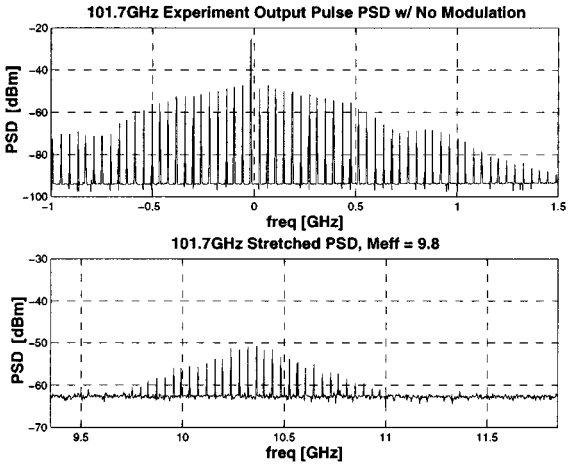

Fig. 6. Stretch experiment with 101.7-GHz Klystron source. Top trace is zero-modulation spectrum, differing slightly from Fig. 2 because increasing M from 4 to 11 has changed the pulse shape. Bottom trace shows stretched spectrum with $M_{\text{eff}} = 9.8$. The frequency axes for both plots have the same scaling and span.

It must be noted that time stretching suffers an inherent bandwidth limitation, analogous to defocused imaging in the spatial domain. As calculated in [3], the intensity transmission versus modulation frequency consists of a series of deep notches; a larger M results in a lower first-notch frequency. For this experiment, the narrow-band modulation signals were chosen to avoid the notch frequencies, an unavailable option for a wide-band signal. In an A/D preprocessor application, the actual system bandwidth is limited both by the modulator and the maximum stretch ratio required to map into the A/D converter's operating range.

Acknowledgment

The authors would like to thank I. Poberezhskiy, Drs. B. Tsap and Y. Chang, H. Zhang, Drs. F. Coppinger and B. Jalali, and A. S. Bhushan for their assistance.

References

[1] D. Chen, H. R. Fetterman, A. Chen, W. H. Steier, L. R. Dalton, W. Wang, and Y. Shi, "Demonstration of 110 GHz electro-optic polymer modulators," *Appl. Phys. Lett.*, vol. 70, no. 25, pp. 3335–3337, 1997.

[2] M. C. Oh, H. Zhang, A. Szep, V. Chuyanov, W. H. Steier, C. Zhang, and L. R. Dalton, "Practical electro-optic polymer modulators using PC/CLD," in *Organic Thin Films for Photonic Applications*, Sept 1999.

[3] F. Coppinger, A. S. Bhushan, and B. Jalali, "Photonic time stretch and its application to analog-to-digital conversion," *IEEE Trans. Microwave Theory Tech.*, vol. 47, no. 7, pp. 1309–1314, 1999.

[4] C. V. Bennet and B. H. Kolner, "Upconversion time microscope demonstrating 103X magnification of femtosecond waveforms," *Opt. Lett.*, vol. 24, no. 11, pp. 783–785, June 1999.

[5] C. V. Bennett, R. P. Scott, and B. H. Kolner, "Temporal magnification and reversal of 100 Gb/s optical data with an up-conversion time microscope," *Appl. Phys. Lett.*, vol. 65, no. 20, pp. 2513–2515, Nov. 1994.

[6] W. J. Caputi, "Stretch: A time-transformation technique," *IEEE Trans. Aerosp. Electron. Syst.*, vol. AES-7, pp. 269–278, March 1971.

[7] B. H. Kolner, "Space–time duality and the theory of temporal imaging," *IEEE J. Quantum Electron.*, vol. 30, pp. 1951–1963, Aug. 1994.